mTOR kinase inhibitors promote antibody class switching via mTORC2 inhibition

Jose J. Limon[a,b], Lomon So[a,b], Stefan Jellbauer[b,c], Honyin Chiu[a,b], Juana Corado[a], Stephen M. Sykes[d], Manuela Raffatellu[b,c], and David A. Fruman[a,b,1]

[a]Department of Molecular Biology & Biochemistry, [b]Institute for Immunology, and [c]Department of Microbiology & Molecular Genetics, University of California, Irvine, CA 92697; and [d]Fox Chase Cancer Center, Philadelphia, PA 19111

Edited by Kevan M. Shokat, University of California, San Francisco, CA, and approved October 22, 2014 (received for review April 18, 2014)

The mammalian target of rapamycin (mTOR) is a kinase that functions in two distinct complexes, mTORC1 and mTORC2. In peripheral B cells, complete deletion of mTOR suppresses germinal center B-cell responses, including class switching and somatic hypermutation. The allosteric mTORC1 inhibitor rapamycin blocks proliferation and differentiation, but lower doses can promote protective IgM responses. To elucidate the complexity of mTOR signaling in B cells further, we used ATP-competitive mTOR kinase inhibitors (TOR-KIs), which inhibit both mTORC1 and mTORC2. Although TOR-KIs are in clinical development for cancer, their effects on mature lymphocytes are largely unknown. We show that high concentrations of TOR-KIs suppress B-cell proliferation and differentiation, yet lower concentrations that preserve proliferation increase the fraction of B cells undergoing class switching in vitro. Transient treatment of mice with the TOR-KI compound AZD8055 increased titers of class-switched high-affinity antibodies to a hapten–protein conjugate. Mechanistic investigation identified opposing roles for mTORC1 and mTORC2 in B-cell differentiation and showed that TOR-KIs enhance class switching in a manner dependent on forkhead box, subgroup O (FoxO) transcription factors. These observations emphasize the distinct actions of TOR-KIs compared with rapamycin and suggest that TOR-KIs might be useful to enhance production of class-switched antibodies following vaccination.

kinase | B lymphocyte | rapamycin | class switching | differentiation

B-cell activation by antigen leads to clonal expansion, followed by differentiation into plasma cells secreting antigen-specific antibodies. Early in an immune response, some B cells differentiate rapidly into plasmablasts that secrete antibodies that are mostly of the IgM isotype and of low affinity. Other B cells adopt a germinal center (GC) fate and undergo class switch recombination (CSR) and somatic hypermutation. Ultimately, GC B cells that survive selection become plasma cells secreting high-affinity antibodies of various isotypes or become long-lived memory B cells.

Extracellular inputs including B-cell receptor engagement, Toll-like receptor ligation, and cytokines, all activate the signaling enzyme phosphoinositide 3-kinase (PI3K) and its downstream target AKT (also known as protein kinase B) in B cells (1). PI3K/AKT signaling and other inputs activate the mammalian target of rapamycin (mTOR), a multifunctional kinase that promotes cell growth, division, and metabolic reprogramming (1, 2). The mTOR kinase is present in two cellular complexes, mTOR-complex 1 (mTORC1) defined by the raptor subunit and mTOR-complex 2 (mTORC2) defined by rictor (3). The classical mTOR inhibitor rapamycin forms a complex with FKBP12 that partially inhibits mTORC1 and can disrupt mTORC2 assembly upon prolonged cellular exposure. mTORC1 acts downstream of AKT and other signals to promote biosynthetic processes essential for cell growth and division. mTORC2 acts upstream of AKT by phosphorylating Ser-473 in the AKT hydrophobic motif. mTORC2 and AKT function are required for subsequent phosphorylation of forkhead box, subgroup O (FoxO) transcription factors (4, 5). When phosphorylated, FoxO factors exit the nucleus and transcription of FoxO target genes is reduced.

Recent studies illustrate the complexity of mTOR function in B cells. Conditional deletion of the mTOR gene in mouse B cells strongly impairs proliferation and GC differentiation (6). Inactivation of mTORC2 in B cells, via rictor deletion, reduces mature B-cell survival and impairs antibody responses and GC formation (7). At concentrations above 1 nM, rapamycin markedly impairs proliferation of both mouse and human B cells and suppresses antibody responses (8, 9). However, at lower concentrations that preserve B-cell proliferation, rapamycin still suppresses class switching but unexpectedly promotes IgM responses that provide heterosubtypic protection from influenza (6, 10). These studies suggest that overall mTOR signaling, as well as the relative activity of mTORC1 and mTORC2, controls the ability of B cells to divide and to differentiate.

ATP-competitive mTOR kinase inhibitors (TOR-KIs) block activity of both mTORC1 and mTORC2, and were developed to overcome limitations of rapamycin as anticancer agents (11, 12). We reported that TOR-KIs do not block proliferation of normal mature B cells at concentrations that cause cell cycle arrest in pre-B leukemia cells (9). However, the impact of TOR-KIs on immune function is still poorly characterized. In this study, we tested whether TOR-KIs can skew the differentiation of activated B cells. We found that partial mTORC1/mTORC2 inhibition or mTORC2 deletion increases CSR, whereas selective inhibition of mTORC1 suppresses CSR.

Significance

Rapamycin is an immunosuppressive drug that partially inhibits the cellular kinase mammalian target of rapamycin (mTOR). This study uncovers previously unidentified mechanisms of mTOR signaling in B cells. Antigen recognition and other signals activate mTOR, a central driver of lymphocyte proliferation and differentiation. However, mTOR forms two protein complexes (mTORC1 and mTORC2) whose roles in B-cell differentiation are poorly defined. We found that a new class of ATP-competitive mTOR kinase inhibitors (TOR-KIs) can augment antibody class switching at concentrations that partially inhibit mTOR activity. Mechanistic studies indicate that mTORC1 loss suppresses, whereas mTORC2 loss promotes, class switching. The dominant effect of TOR-KIs is to promote switching through mTORC2 inhibition. These findings establish distinct immunomodulatory activity of TOR-KIs compared with the canonical mTOR inhibitor rapamycin.

Author contributions: J.J.L., L.S., S.J., H.C., S.M.S., M.R., and D.A.F. designed research; J.J.L., L.S., S.J., H.C., J.C., and S.M.S. performed research; S.M.S. contributed new reagents/analytic tools; J.J.L., L.S., S.J., H.C., J.C., M.R., and D.A.F. analyzed data; and J.J.L., L.S., S.J., H.C., S.M.S., M.R., and D.A.F. wrote the paper.

The authors declare no conflict of interest.

This article is a PNAS Direct Submission.

[1]To whom correspondence should be addressed. Email: dfruman@uci.edu.

This article contains supporting information online at www.pnas.org/lookup/suppl/doi:10.1073/pnas.1407104111/-/DCSupplemental.

Results

High Concentrations of TOR-KIs Block B-Cell Proliferation. We reported previously that the TOR-KI compound PP242, when added at a concentration of 100 nM, fully suppresses mTOR signaling in B cells without blocking proliferation (9). This result was surprising because the allosteric mTOR inhibitor rapamycin had only partial effects on signaling yet fully blocked B-cell proliferation (9). Our initial signaling measurements were taken 15 min after B-cell stimulation (9), so we speculated that the effects of PP242 might be transient and wear off before the cell commits to division. To test this idea, we conducted a time course measuring phosphorylation of the ribosomal S6 protein at the Ser-240/244 site (p-S6), which is a sensitive readout of mTORC1 activity. Consistent with our prediction, 100 nM PP242 blocked p-S6 to near completion at 3 h after B-cell stimulation but much less at 24 and 48 h (Fig. 1 *A* and *B*). By 48 h, the cells had proliferated nearly to the same extent as control vehicle-treated B cells, as assessed by carboxyfluorescein succinimidyl ester (CFSE) dilution (Fig. 1*B*). In contrast, increasing the concentration of PP242 to 400 nM caused sustained inhibition of p-S6 and blocked proliferation similar to cells treated with 10 nM rapamycin. Based on these results, in subsequent B-cell differentiation experiments, we used PP242 and other TOR-KIs at concentrations that have a minimal impact on proliferation (Fig. 2 *A* and *D* and Fig. S1*A*) and partially reduce phosphorylation of mTORC1 and mTORC2 substrates at 24 h (Fig. S1*B*).

TOR-KIs Increase B-Cell Isotype Switching in Vitro. In a previous study, we administered PP242 to mice and assessed the effect on antibody responses to the T cell-dependent (TD) antigen nitrophenyl-ovalbumin (NP-OVA) (9). We found that PP242 did not strongly suppress NP-specific IgM or IgG1 and caused a significant increase in the percentage of B cells with a GC phenotype in some experiments (9). To define the B cell-intrinsic effects of TOR-KIs further, we assessed the differentiation of purified splenic B cells. We used four different TOR-KIs with distinct chemical structures (INK128, PP242, Ku-0063794, and AZD8055) to minimize the potential for off-target effects. Each compound increased the percentage of IgG1-switched $B220^+$ B cells induced by anti-CD40 plus IL-4, a condition that mimics signals during a TD response and favors isotype switching to IgG1 (Fig. 2 *A* and *B*). Direct inhibition of AKT isoforms AKT1 and AKT2 also increased the frequency of switching to IgG1 (Fig. 2 *A* and *B*). Similar results were observed when B cells activated by LPS plus IL-4 were treated with INK128, PP242, Ku-0063794, or AZD8055 (Fig. 2*C*). Consistent with increased switching to the IgG1 isotype, postrecombination Iμ-Cγ1 transcripts were increased in B cells treated with TOR-KIs (Fig. S2). In addition, TOR-KI–treated B cells displayed an elevation in *Aicda* transcripts encoding activation-induced cytidine deaminase (Fig. 2*G*), the mutator protein required for initiation of CSR (13).

As reported previously (14, 15), inhibiting PI3K strongly induced switching to IgE with lesser effects of AKT inhibition (Fig. S3). Under these conditions, TOR-KIs had minimal effects on switching to IgE, an isotype important for allergic responses (Fig. S3). Hence, the enhanced switching to IgG1 caused by TOR-KIs is distinct from the IgE increases caused by PI3K inhibition.

We next assessed the effect of TOR-KIs on differentiation into plasmablasts and antibody-secreting cells (ASCs) following stimulation with LPS. Plasmablast differentiation, as measured by cells with a $B220^{low}CD138^+$ phenotype, was decreased in a concentration-dependent manner by TOR-KIs, whereas AKT inhibition had no significant effect (Fig. 2 *D* and *E*). TOR-KIs also reduced IgM production, as measured by ELISA from cell culture supernatants of LPS-stimulated B cells (Fig. 2*F*). Thus, our results demonstrate that TOR-KIs can directly alter B-cell differentiation fate, causing increased CSR and a reciprocal decrease in plasmablast and ASC differentiation.

In contrast to the effects of TOR-KIs, rapamycin reduced both CSR and ASC differentiation (Fig. 2). The suppression of both differentiation pathways is consistent with early studies of rapamycin action in B cells (8).

TOR-KIs Promote High-Affinity IgG1 Production in Vivo. To extend these observations to an in vivo system, we assessed the effect of TOR-KIs on B-cell responses in mice. Chronic treatment of mice with TOR-KIs did not increase antigen-specific IgG or IgM production consistently (9) (Fig. S4). We reasoned that continuous

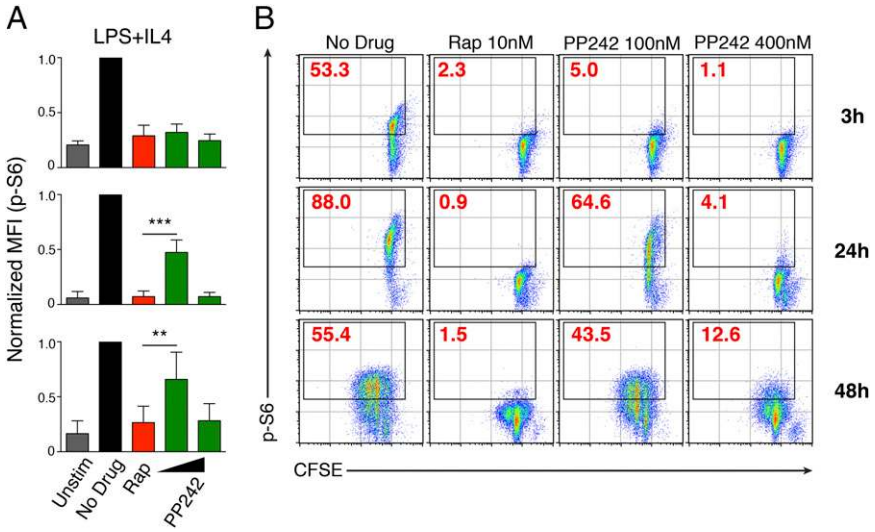

Fig. 1. High concentrations of TOR-KIs reduce mTORC1 activity and block B-cell proliferation. (*A* and *B*) Purified splenic B cells were labeled with CFSE to track cellular proliferation and cultured with media only or stimulated with LPS + IL-4 or LPS + IL-4 and inhibitors at the indicated concentrations. (*A*) mTORC1 activity was assessed at the indicated time points (*B*, *Far Right*) by intracellular staining (ICS) for p-S6 (S240/244 site) on proliferated cells. The graphs depict mean ± SEM of the p-S6 [median fluorescence intensity (MFI)] ($n = 3$). Data were normalized to the stimulated, no-drug treatment condition. (**$P < 0.01$, one-way ANOVA with Tukey's multiple comparison test). Unstim, unstimulated. (*B*) CFSE-labeled B cells were stimulated with LPS + IL-4 without or with inhibitors at the indicated concentrations for 48 h. Data are representative of three independent experiments. Rap, rapamycin.

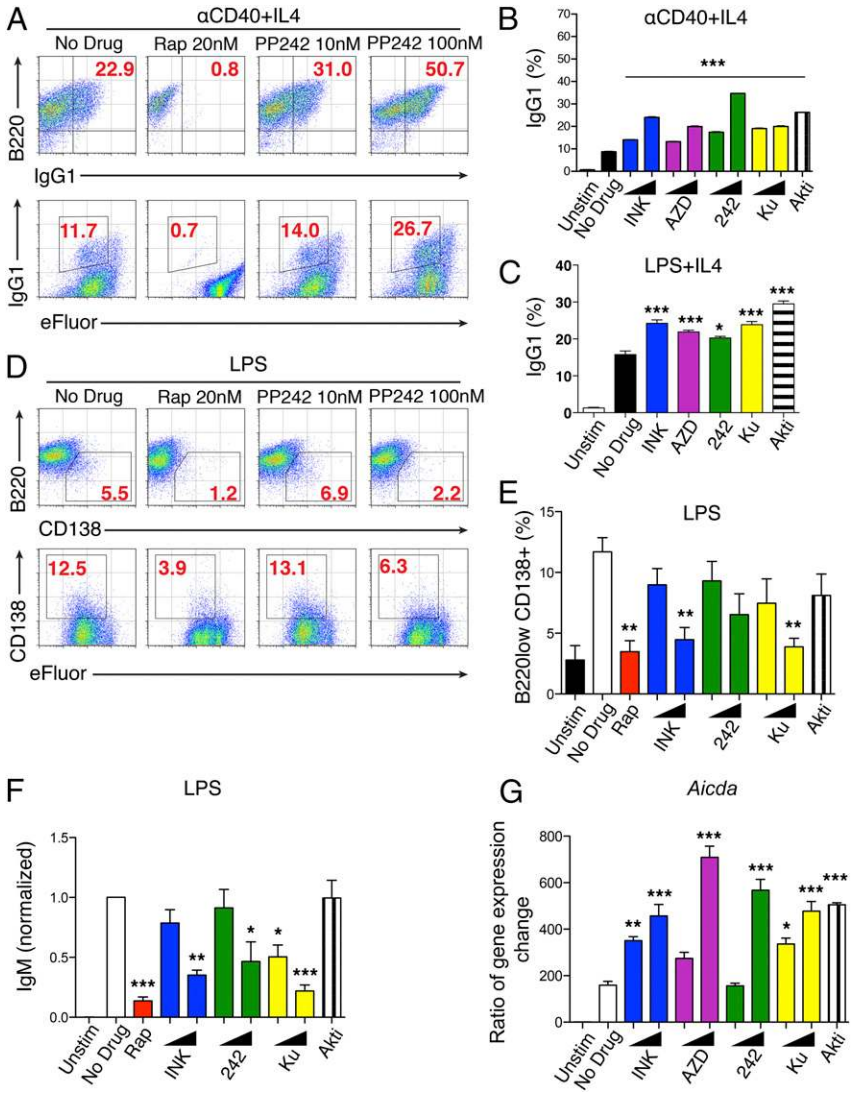

Fig. 2. TOR-KIs increase in vitro B-cell CSR and decrease plasmablast differentiation. (*A* and *B*) Purified B cells were cultured with media only or stimulated with αCD40 + IL-4 in the absence or presence of the inhibitors indicated. (*A*) Dot plots show IgG1$^+$ B cells (*Top*) and the cell division history of eFluor670-labeled B cells (*Bottom*; eFluor670 is a cell division tracking dye with a different emission spectrum than CFSE), as determined by FACS after 4 d. Other TOR-KIs in this study had similar effects on cell division at the concentrations used for differentiation experiments. (*B*) Percentage of live B cells that have divided at least once (based on eFluor670 division history) expressing surface IgG1 was determined by FACS after 4 d. (*C*) Switching to IgG1 was assessed as in *B*, except cells were stimulated with LPS + IL-4. (*D*) Representative FACS plots of plasmablast differentiation in purified B cells stimulated with LPS or LPS and indicated inhibitors for 3 d. (*Bottom*) B cells were labeled with eFluor670 to track division history. (*E*) Graph of the percentage of live B cells with a plasmablast phenotype determined by FACS after 3 d of stimulation as indicated in *D*. (*F*) Purified B cells were stimulated with LPS in the absence or presence of the inhibitors indicated. The amount of IgM in cell supernatants was quantitated by ELISA after 4 d, and data were normalized to the stimulated, no-drug treatment condition. (*G*) *Aicda* mRNA transcripts were quantitated by qPCR in B cells stimulated with αCD40 + IL-4. For *A* and *D*, data are representative of three or more independent experiments. For *B*, *C*, *E*, *F*, and *G*, graphs depict the mean and SEM of $n \geq 3$ samples per condition. (*$P < 0.05$; **$P < 0.01$; ***$P < 0.001$ by one-way ANOVA with Tukey's multiple comparison test, measured vs. the no-drug sample). Akti, Akt inhibitor VIII; AZD, AZD8055; INK, INK128; Ku, Ku-0063794; 242, PP242.

treatment might suppress terminal differentiation of GC cells into plasma cells. Therefore, we tested whether transient TOR-KI administration can enhance antibody responses in vivo.

Of the inhibitors tested in vitro (Fig. 2 *B* and *C*), we chose AZD8055 for most in vivo experiments because it is well tolerated at a dose with anticancer activity in mice (20 mg·kg^{-1}·d^{-1}) (16, 17). Mice were treated daily for a total of 4 d with AZD8055 or vehicle alone, beginning the day before immunization and stopping 2 d postimmunization (PID 2). Immunization with NP-OVA was performed on PID 0, and mice were boosted on PID 21, thus allowing for the interrogation of both primary and secondary humoral immune responses. Transient AZD8055 treatment significantly increased primary NP-specific IgG1 antibody titers at PID 21 ($P < 0.05$) (Fig. 3*A*). Secondary responses measured 7 d after antigen boosting (PID 28) were also augmented in AZD8055-treated mice (Fig. 3*A*). Transient AZD8055 treatment also significantly increased the production of high-affinity anti-NP antibody in the primary and secondary responses (Fig. 3*B*). Similar results were observed in a separate cohort of mice treated transiently with INK128 before and after NP-OVA immunization (Fig. S5).

Augmented B-cell class switching could be driven, in part, by drug effects on non-B cells in vivo. For example, the differentiation of follicular helper T (T_{FH}) cells is known to be influenced by PI3K activity (18). Interestingly, mice in the AZD8055 treatment group showed an increase in T_{FH}-cell percentages, as measured

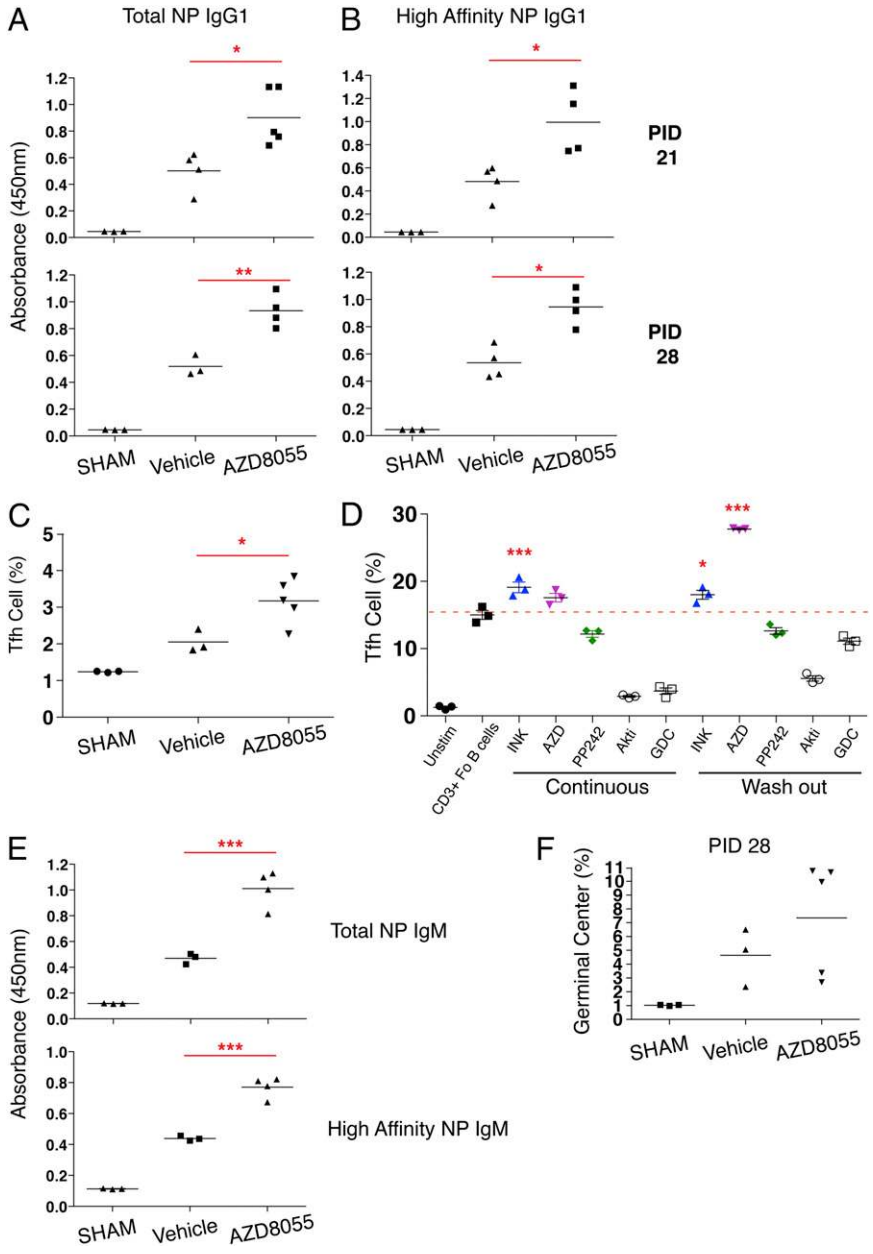

Fig. 3. Transient treatment with AZD8055 increases class-switched antibody responses in vivo. Mice were immunized with NP-OVA and treated daily for 4 d with AZD8055 at 20 mg/kg (PID −1 to PID 2). (*A* and *B*) Total and high-affinity NP-specific IgG1 production was measured by ELISA in sera collected during both the primary (PID 21) and secondary (PID 28) immune responses. (*C*) Percentage of spleen cells with a T_{FH} phenotype ($CD4^+CXCR5^{high}PD\text{-}1^+$) was determined by FACS at PID 28. (*D*) Purified $CD4^+$ T cells were cultured under skewing conditions and restimulated to determine the percentage of cells producing cytokines characteristic of T_{FH} cells ($IL\text{-}21^+IL\text{-}17A^-$). Cells were cultured in the continuous presence of inhibitors (*Left*) or for 24 h with inhibitors, followed by washout of drug from the cultures (*Right*). (*E*) Total and high-affinity NP-specific IgM was measured at PID 28. (*F*) Percentage of spleen cells with a GC phenotype ($B220^+$, IgD^{low}, $CD38^-$, and Fas^+) was determined by FACS at PID 28. (*$P < 0.05$; **$P < 0.01$; ***$P < 0.001$ by one-way ANOVA with Tukey's multiple comparison test, measured vs. the vehicle group).

by a $CD4^+$ C-X-C chemokine receptor type 5-high ($CXCR5^{high}$) programmed cell death protein 1-positive ($PD1^+$) immunophenotype (Fig. 3*C*). Treatment of CD4 T cells with the TOR-KIs AZD8055 and INK128 in vitro potentiated T_{FH} cell differentiation, whereas PI3K or AKT inhibitors suppressed T_{FH}-cell percentages (Fig. 3*D*). The effect of AZD8055 was significantly stronger when the drug was removed from the culture after 24 h (Fig. 3*D*). Thus, the ability of TOR-KIs to promote class switching may involve increased T_{FH}-cell differentiation.

Next, we evaluated other parameters of B-cell differentiation at PID 28. Transient AZD8055 treatment increased production of NP-specific IgM in the secondary response, including high-affinity IgM (Fig. 3*E*). This result suggests that transient pharmacological inhibition of mTOR does not block terminal differentiation of IgM-secreting plasma cells, and might instead lead to increased output of post-GC cells secreting high-affinity IgM. At PID 28, the percentage of GC B cells was not significantly increased in AZD8055-treated animals compared with the vehicle control group (Fig. 3*F*). To gain a preliminary assessment of memory B-cell formation, we enumerated the percentage of $B220^+$, IgD^-, surface $IgG1^+$ NP-binding cells at PID 28. As expected, vehicle-treated immunized animals showed a trend

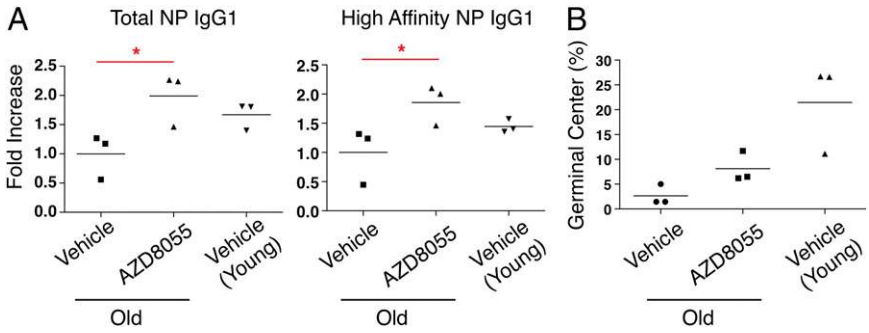

Fig. 4. Transient treatment with AZD8055 improves the humoral response in aged mice in vivo. Aged mice (~1.5 y old) were transiently treated with AZD8055 as described above and immunized with NP-OVA. (*A*) Production of total and high-affinity NP-specific IgG1 was measured by ELISA, with vehicle-treated young immunized mice as a comparison. (*B*) Percentage of spleen cells with a GC phenotype was determined by FACS at PID 28. (*$P < 0.05$, one-way ANOVA with Tukey's multiple comparison test, measured vs. the vehicle group.)

toward increased NP-binding IgG1$^+$ cells compared with sham-immunized controls at this time point (mean = 0.35 ± 0.07% vs. 0.19 ± 0.09%; $P = 0.06$). The percentage of NP-binding IgG1$^+$ cells was significantly increased in the AZD8055-treated group (mean = 0.54 ± 0.07%; $P < 0.05$ vs. vehicle). Together, these data show that transient TOR-KI treatment, starting 1 d before and ending 2 d after immunization with a TD antigen, improves the outcome of the humoral immune response. Specifically, TOR-KI–treated mice show higher titers and affinity of antigen-specific class-switched antibody and generate an increased percentage of B cells with a memory phenotype.

Next, we assessed the antibody response to a live-attenuated strain of *Salmonella* Typhimurium. The early humoral response to *Salmonella* in C57BL/6 mice is dominated by IgM antibodies and an extrafollicular IgG2c response, with GCs delayed until several weeks after infection (19, 20). In C57BL/6 mice infected with a vaccine strain of *Salmonella*, transient treatment with AZD8055 starting the day before immunization was poorly tolerated. We then switched to a protocol in which mice were treated during days 3–6 after immunization. Under these conditions, AZD8055 did not alter the early IgM response or induce IgG3 production at day 14 postinfection (Fig. S6*A*), whereas it decreased early IgG2c production. However, by day 29 post-infection, there was a significant increase in *Salmonella*-specific antibodies of IgM isotype, increased IgG3 in three of four mice, and no difference in IgG2c isotype (Fig. S6*B*). At day 29 post-infection, the percentage of T_{FH} cells was also increased in AZD8055-treated mice, and two mice in this group had elevated GC B-cell percentages (Fig. S6*C*). Further work is needed to identify conditions in which TOR-KIs strongly improve antibody production to pathogens and vaccines; nevertheless, the in vivo data largely recapitulate our in vitro findings.

TOR-KIs Improve Antibody Responses in Aged Mice. Age-related decreases in immune function can be attributed to defects in the innate and adaptive immune compartments, including humoral immunity (21). Therefore, we assessed the impact of AZD8055 on in vivo humoral responses to NP-OVA in aged mice, using the transient dosing protocol as described above. We observed a reduction in NP-specific IgG1 in aged mice compared with young mice, which was largely reversed by AZD8055 treatment (Fig. 4*A*). Total and high-affinity NP-specific IgG1 antibody titers from AZD8055-treated mice 7 d after boosting were statistically significant ($P < 0.05$) vs. the vehicle-treated group (Fig. 4*A*). These data provide evidence that TOR-KI treatment in the vaccine setting may help correct age-related defects in CSR and help improve humoral immune responses in the elderly. Similar to young AZD8055-treated mice, the percentage of GC B cells was not significantly increased at PID 28 in AZD8055-treated aged mice (Fig. 4*B*).

Rapamycin Reduces CSR by a Mechanism Partly Independent of Proliferation. To gain further insight into the mechanism of mTOR inhibitor action, we measured B-cell proliferation and IgG1 class switching over an extended dose–response of rapamycin or INK128 (Fig. 5). The partial mTORC1 inhibitor rapamycin reduced CSR at concentrations as low as 0.02 nM, with complete inhibition achieved by 0.4 nM. INK128 enhanced CSR at 10 nM, but higher concentrations caused increasing inhibition. Notably, rapamycin ablated CSR even at a concentration (0.4 nM) that partially preserved proliferation, whereas some B cells treated with a high concentration of INK128 (100 nM) still switched to IgG1 even without proliferation. Thus, the roles of mTORC1 and mTORC2 in cell division are partly independent of their roles in differentiation.

Inactivation of mTORC1 vs. mTORC2 Has Opposing Effects on CSR. As a genetic approach to assess the roles of mTORC1 and mTORC2, we isolated B cells from mice possessing conditional (floxed) alleles of rictor or raptor. Deletion of rictor using CD19Cre (rictor-flox/CD19Cre; termed rictor$^{\Delta B}$) did not significantly alter B-cell subset frequencies (Fig. S7*A*). In resting mature B cells, rictor expression was not completely reduced, suggesting incomplete and/or ongoing deletion (Fig. 6*A*). Consistent with reduced mTORC2 function, AKT phosphorylation at S473 was lower in B cells from rictor$^{\Delta B}$ mice (Fig. 6*A*). Importantly, this effect was specific to mTORC2, because S6 phosphorylation, a sensitive readout of mTORC1, was unaffected in rictor$^{\Delta B}$ B cells (Fig. 6*A*). To address the role of mTORC1, we analyzed B cells from raptor$^{\Delta B}$ mice in which the raptor-flox allele is deleted at the transitional B-cell stage using CD21Cre. As with rictor$^{\Delta B}$, B-cell development was largely normal in raptor$^{\Delta B}$ (Fig. S7*B*). Raptor expression was also not completely reduced in resting mature B cells (Fig. 6*D*), and this partial deletion corresponded to a reduced but not complete reduction in S6 phosphorylation in raptor$^{\Delta B}$ B cells (Fig. 6*D*).

Next, we tested functional responses in B cells with partial loss of rictor or raptor. In response to anti-CD40 plus IL-4, rictor-deficient B cells proliferated to a similar degree as WT, whereas raptor-deficient cells proliferated less (Fig. 6 *B* and *E*). To compare the capacity of cells to undergo class switching, we gated on divided cells and calculated the percentage of IgG1$^+$ cells. The results showed consistently less switching in divided raptor$^{\Delta B}$ B cells compared with control (Fig. 6*F*). These findings are consistent with the effects of rapamycin on B-cell division and differentiation (Fig. 5). In contrast, rictor$^{\Delta B}$ B cells showed significantly more switching to IgG1 than control (Fig. 6*C*). Importantly,

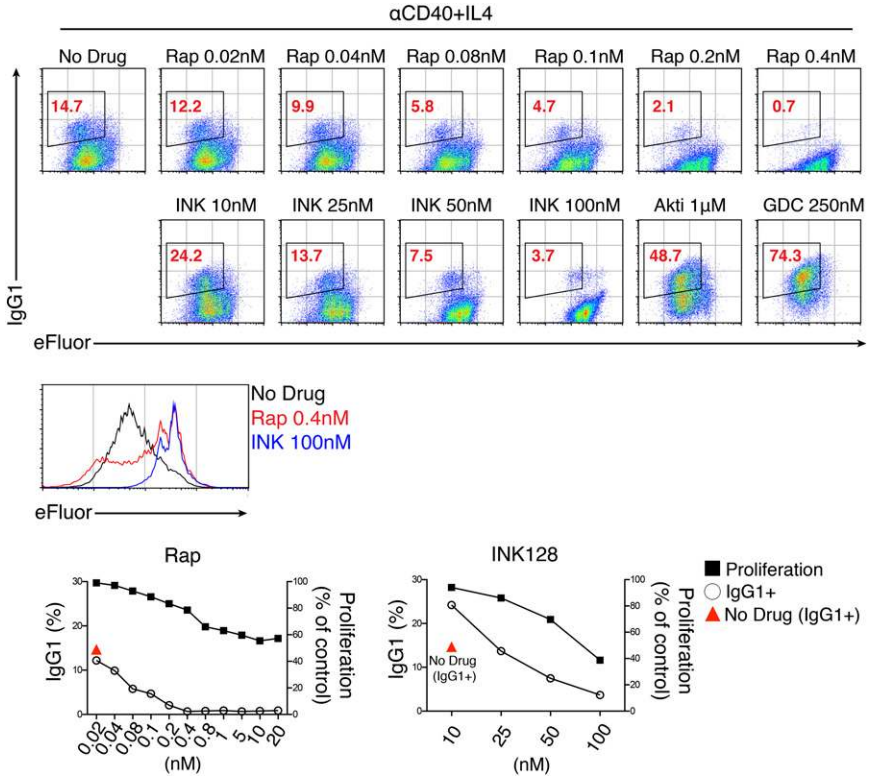

Fig. 5. Rapamycin has a more profound effect on B-cell proliferation and CSR than TOR-KIs. Purified B cells were labeled with eFluor670 to measure cell division and were stimulated with αCD40 + IL-4 in the presence or absence of indicated inhibitors. Representative FACS plots are shown for the different treatment conditions (*Upper*), and a FACS proliferation histogram is shown for high-dose rapamycin and INK128 (*Middle*). (*Lower*) Effects of inhibitor concentration on cellular proliferation and CSR are represented on line graphs. Data are representative of two independent experiments.

adding low-dose TOR-KI (1–5 nM INK128) to rictor$^{\Delta B}$ B cells did not further increase CSR (Fig. 6*C*).

We also measured plasmablast generation in B cells stimulated with LPS alone. The raptor$^{\Delta B}$ B cells showed reduced ASC generation, whereas the rictor$^{\Delta B}$ B cells were similar to control (Fig. 6 *C* and *F*). Together, these genetic interventions support the conclusion that mTORC1 inhibition suppresses both CSR and plasmablast generation, whereas mTORC2 inhibition increases CSR with little effect on plasmablast generation.

FoxO Is Required for TOR-KI–Mediated Increases in CSR. FoxO transcription factors are phosphorylated and inactivated by AKT and by serum- and glucocorticoid-regulated kinases (SGKs) in a manner dependent on mTORC2 (4, 5). Considering that FoxO factors are required for class switching (22), it is possible that TOR-KIs increase CSR through a FoxO-dependent mechanism. To test this possibility, we measured differentiation in B cells lacking FoxO1, FoxO3a, and FoxO4. Mice bearing floxed alleles of *Foxo1*, *Foxo3a*, and *Foxo4* and the inducible Mx1-Cre transgene (23, 24) were injected two times with polyinosinic:polycytidylic acid (polyI:C) before purification of splenic B cells. As a control, we confirmed that TOR-KIs increased IgG1 switching in B cells from polyI:C-treated FoxO triple-floxed mice lacking Mx1-Cre (Fig. S8). In cells from Mx1-Cre^{+} mice, intracellular staining for FoxO1 protein expression revealed incomplete deletion, with ~50% of B220^{+} cells showing low FoxO1 expression (Fig. 7*A*). The presence of a mixed population allowed us to compare differentiation in *Foxo1*-deficient (FoxO1-low) and *Foxo1*-sufficient (FoxO1-high) cells within the same culture (Fig. 7*A*). Fig. 7*B* shows that TOR-KI treatment caused a concentration-dependent increase in IgG1-switched cells among the FoxO1-high population, consistent with the effects in WT B cells and Mx1-Cre^{-} cells. Strikingly, FoxO depletion caused a nearly complete block in IgG1 switching in vehicle-treated cells and prevented the CSR increase in TOR-KI–treated cells (Fig. 7*B*). FoxO1-low cells also did not increase CSR when treated with the AKT1/2 inhibitor or with a pan-PI3K inhibitor, GDC-0941. The latter observation is consistent with the finding that the PI3K p110δ inhibitor IC87114 does not increase CSR in *Foxo1*-deficient B cells under IgG1 switching conditions (22). These data reconfirm the role of FoxO transcription factors in basal CSR and provide further evidence that TOR-KI–mediated CSR enhancement is through the AKT-FoxO signaling axis.

Discussion

TOR-KIs are a powerful new class of compounds that inhibit both rapamycin-sensitive and rapamycin-resistant mTOR functions. These agents not only have great promise for clinical management of cancer but also represent new chemical tools for probing the function of mTOR kinase activity in various cell types. Here, we have used a panel of chemically distinct TOR-KIs to demonstrate that mTOR kinase inhibition increases the fraction of activated B cells undergoing antibody class switching. These results were seen at TOR-KI concentrations that cause transient mTORC1/2 inhibition and only partially reduced signaling after 24 h in B cells. The effect of AKT inhibition or partial mTORC1/2 inhibition to increase CSR requires FoxO transcription factors. In addition, the expression of *Aicda* in activated B cells is known to be FoxO1-dependent (22), and *Aicda* mRNA was increased in cells treated with TOR-KIs or AKT inhibitor. These data support the model that mTORC2 inhibition by TOR-KIs reduces AKT activity, increasing FoxO activity to drive the enhanced class-switching response in TOR-KI–treated B cells (Fig. 8). This model is consistent with previous

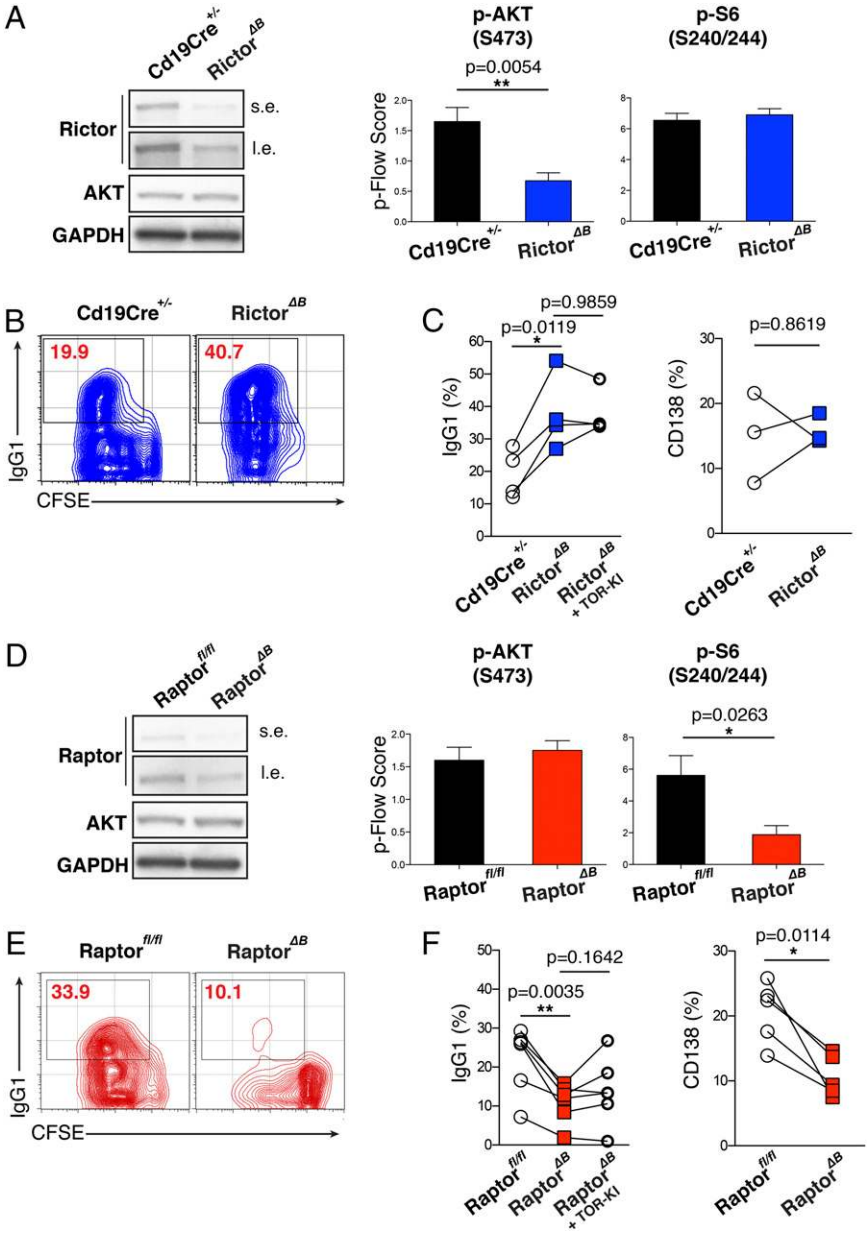

Fig. 6. Inactivation of mTORC1 vs. mTORC2 has opposing effects on CSR. (*A*) Purified resting B cells from either control (CD19Cre$^{+/-}$) or rictor-flox/CD19Cre (rictor$^{\Delta B}$) were subjected to Western blotting to check rictor protein levels (*Left*). RBC-lysed total splenocytes from the indicated genotypes were activated with αCD40 + IL-4 for 24 h, and intracellular phosphoflow (p-Flow) analysis was performed to measure mTORC1 (pS6-S240/244) and mTORC2 (pAKT-S473) activity. The fold change in median fluorescence intensity was calculated and subjected to $\log_2$ conversion to obtain p-Flow score values as previously described (9). Data are reported as mean ± SD [$n = 3$ (pAKT) or $n = 2$ (pS6)]. An unpaired Student *t* test was used for statistical analysis of the pAKT data. l.e., long exposure; s.e., short exposure. (*B*) Purified B cells were labeled with CFSE and activated with αCD40 + IL-4 for 4 d. The percentage of live B cells that had divided at least once (based on CFSE division history) expressing surface IgG1 was determined by FACS after 4 d. (*C*, *Left*) Percentage of B cells expressing surface IgG1 after 4 d of activation with αCD40 + IL-4 is plotted for several experiments. In the +TOR-KI condition, INK128 was added at a concentration of 1–5 nM. (*C*, *Right*) Percentage of B cells expressing surface CD138 after 4 d of activation with LPS is plotted. (*D*, *Left*) Western blotting was performed the same way as in *A* but with resting B cells from control (raptor$^{fl/fl}$) or raptor-flox/CD21Cre (raptor$^{\Delta B}$). (*D*, *Right*) Intracellular p-Flow analysis to measure mTORC1 and mTORC2 activity after 24 h of αCD40 + IL-4 activation. Data are reported as mean ± SD ($n = 3$) for both pAKT and pS6. An unpaired Student *t* test was used for statistical analysis. (*E*) Representative FACS plots as in *B*. (*F*) Same analysis as in *C*. A paired Student *t* test was used for statistical analysis of both *C* and *F*.

studies showing that PI3K activity suppresses CSR through AKT-dependent inactivation of FoxO1, whereas PI3K inhibition or FoxO activation promotes CSR (22, 25).

The enhanced production of class-switched antibodies by mTORC1/mTORC2 inhibition is surprising, considering the well-known immunosuppressive activity of rapamycin and the impaired survival and differentiation of mouse B cells lacking mTOR (6). Our in vitro studies establish the importance of using intermediate doses of competitive mTOR inhibitors that transiently inhibit both mTORC1 and mTORC2. At higher concentrations, TOR-KIs sustain mTOR inhibition and block B-cell proliferation to a similar degree as rapamycin, probably through strong mTORC1 inhibition (Fig. 8). Supporting the model that TOR-KIs increase CSR via mTORC2 inhibition, genetic loss of mTORC2 (via partial rictor deletion) causes increased CSR that is not elevated further by TOR-KI treatment. Our findings contrast with a

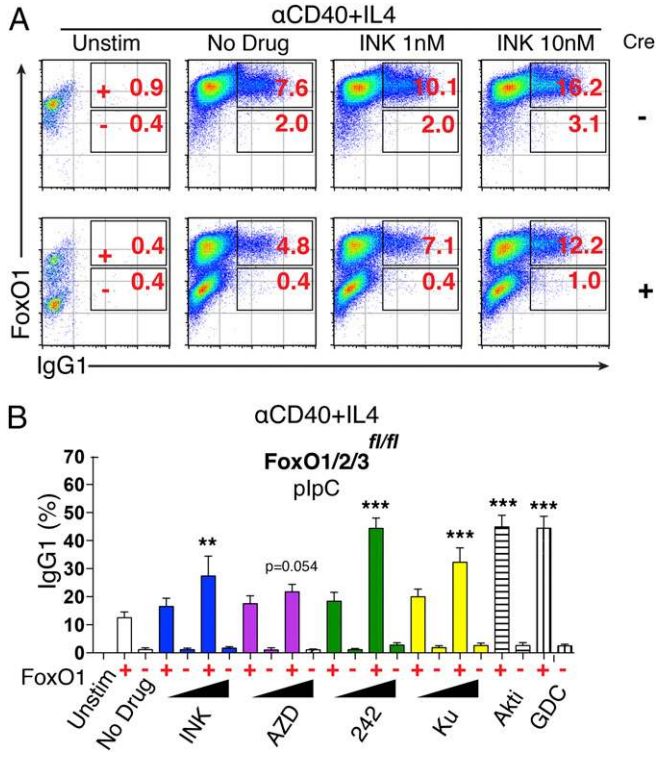

Fig. 7. Increases in B-cell CSR are mediated by FoxO transcription factors. (*A*) Purified B cells from polyI:C-treated FoxO triple-floxed mice lacking Mx1-Cre were treated with the indicated inhibitors, followed by stimulation with αCD40 + IL-4. The percentage of IgG1-switched cells was determined as in Fig. 2. (*A* and *B*) PolyI:C-treated FoxO triple-floxed mice (FoxO1/2/3$^{fl/fl}$) expressing Mx1-Cre were treated with polyI:C and stimulated with αCD40 + IL-4. Intracellular staining was used to distinguish FoxO-deleted cells (indicated by red − signs) from nondeleted cells (indicated by red + signs) in the same population. (*B*) Percentage of IgG1-switched B cells was reported as mean ± SEM (**$P < 0.01$; ***$P < 0.001$ by one-way ANOVA with Tukey's multiple comparison test, measured on FoxO-sufficient cells vs. the no-drug sample). GDC, GDC-0941.

recent report that deletion of rictor in B cells reduces survival and proliferation, and impairs class switching (7). It appears that these systems achieve differential efficiency of rictor deletion. Boothby and coworkers (7) obtained efficient deletion using Vav-Cre, where rictor is deleted in all hematopoietic cells, or using an inducible Cre (fused to the estrogen receptor hormone binding domain) by which chronic in vivo tamoxifen treatment directs rictor deletion in all cell types. We used CD19Cre, which mediated partial deletion of rictor in B cells and partial but not complete loss of mTORC2 signaling. Partial rictor deletion allowed B cells to survive and proliferate, and led to enhanced class switching. The results we obtained with rapamycin titrations are consistent with recent evidence that mTORC1 inhibition can suppress CSR independent of proliferation (10) (Fig. 8). An interesting finding is that when both complexes are partially inhibited by intermediate concentrations of TOR-KIs, the effect of mTORC2 inhibition is dominant for CSR (enhancement), whereas mTORC1 inhibition is dominant for ASC generation (inhibition).

Our findings also demonstrate that TOR-KIs can improve humoral immune responses in vivo. Daily dosing with AZD8055 for a limited time (4 d) increased antigen-specific IgG1 production in young and aged mice immunized with a model antigen. Extended treatment with INK128 did not enhance IgG1 production, possibly resulting from impaired plasma cell differentiation. The in vitro data suggest that TOR-KIs promote CSR, in part, through B cell-intrinsic effects. However, AZD8055 was reported to enhance innate immune activation to promote anticancer immune responses (26); therefore, mTOR inhibition might augment immune responses, in part, through stimulating inflammatory cytokine production (27, 28). In addition, our data show that TOR-KIs can promote T_{FH}-cell differentiation both in vitro and in vivo. Further experiments will be needed to determine the mechanism of enhanced T_{FH} differentiation and how this effect is modulated by different drug doses and schedules.

Overall, our findings emphasize that targeted inhibitors of the PI3K/AKT/mTOR pathway have important immunomodulatory effects at concentrations that do not strongly suppress lymphocyte clonal expansion. Additional studies will be required to determine whether TOR-KIs stimulate faster or more potent antibody responses to different immunogens and with distinct adjuvants and routes of administration. Eventually, TOR-KI treatment could be used to improve vaccine efficacy or to boost the production of class-switched antibodies in animals for biomedical applications.

Materials and Methods

Mice and Reagents. C57BL6 mice were bred at the University of California, Irvine, and used at between 6 and 12 wk of age. Aged mice, 16–18 mo old, on a C56Bl6/SJL mixed background with a transgenic GFP expressed under CD88 promoter were kindly donated by Andrea Tenner (University of California, Irvine). *Raptor*$^{fl/fl}$ mice on a C57BL6 background were obtained from the Jackson Laboratories (stock no. 013138) and have been described previously (29). *Rictor*$^{fl/fl}$ mice on a C57BL6 background were a generous gift from Mark Magnuson (Vanderbilt University, Nashville, TN) and have been

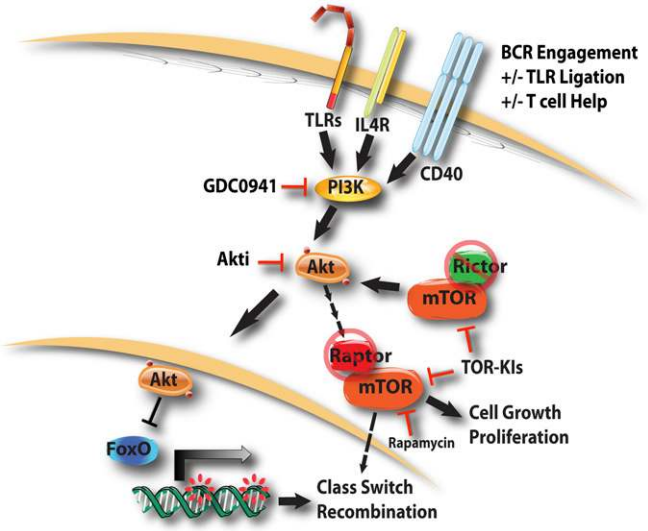

Fig. 8. Roles of mTOR complexes in CSR and the effects of distinct classes of mTOR inhibitors. Activated B cells initiate CSR in response to T cell-derived signals (CD40, IL-4) and/or innate pattern recognition [Toll-like receptor (TLR) engagement]. These signals converge on the lipid kinase PI3K, leading to activation of the Ser/Thr kinase AKT. The predominant action of AKT is to suppress CSR by inactivating FoxO transcription factors that are required for this process (22, 25). Thus, inhibitors of PI3K or AKT tend to increase CSR. mTOR exists in two complexes with complex roles in CSR. mTORC1 (defined by the raptor subunit) promotes CSR through an unknown mechanism (multiple arrows) that is partially independent of the role of mTORC1 in B-cell proliferation. Consequently, deletion of raptor or treatment with the selective mTORC1 inhibitor rapamycin suppresses CSR. mTORC2 (defined by the rictor subunit) suppresses CSR by promoting AKT phosphorylation, leading to FoxO inactivation. Thus, partial deletion of rictor increases CSR. When B cells are treated with TOR-KIs at submaximal concentrations that preserve proliferation, the mTORC2 effect dominates and CSR increases. At higher concentrations, full inhibition of both mTORC1 and mTORC2 suppresses proliferation and CSR. Although AKT can promote mTORC1 activity (multiple arrows), inhibition of PI3K/AKT does not completely suppress mTORC1 signaling in activated B cells (36).

described previously (30). CD21-Cre mice were obtained from the Jackson Laboratories (stock no. 006368). *FoxO1/3/4*$^{fl/fl}$; *Mx1-Cre*$^{+}$ and *FoxO1/3/4*$^{fl/fl}$; *Mx1-Cre*$^{-}$ mice were bred at Harvard Medical School (Boston, MA). All animals were studied in compliance with protocols approved by the Institutional Animal Care and Use Committees of the University of California, Irvine, and Harvard Medical School. The active site mTORC1/2 inhibitors PP242, AZD8055, WYE-354, and Ku-0063794 were purchased from Chemdea, and INK128 was obtained from Intellikine. The p110δ-selective PI3K inhibitor IC87114 and pan-PI3K class I inhibitor GDC-0941 were obtained from Intellikine. The inhibitor of AKT1 and AKT2, Akt inhibitor VIII, was purchased from Chemdea. The mTOR allosteric inhibitor, rapamycin, was purchased from LC Labs.

Primary Cell Culture. Mouse splenic B cells were purified by negative selection using anti-CD43 biotinylated antibody, followed by incubation with anti-biotin magnetic microbeads and separation on MACS columns (Miltenyi Biotec). B-cell purity was >98% as measured by FACS analysis (FACSCalibur and CellQuest software; BD Biosciences) using anti-B220 antibody (BioLegend). Purified B cells were seeded at a final concentration of $0.2 \times 10^{\wedge 6}$ cells per milliliter. For ASC differentiation, B cells were stimulated with 5 μg/mL LPS (Sigma) for 72 h, and for IgG1 CSR, B cells were stimulated with 3 units of CD40L (a gift from Paolo Casali, University of California, Irvine), 1 μg/mL anti-CD40 (HM40-3) agonistic antibody (BioLegend), or 5 μg/mL LPS (Sigma), together with 2.5 ng/mL mIL-4 (R&D Systems) for 96 h. All B cells were cultured in RPMI 1640 supplemented with 10% (vol/vol) heat-inactivated FCS, 5 mM Hepes, 2 mM L-glutamine, 100 units/mL penicillin, 100 μg/mL streptomycin, 50 μM 2-mercaptoethanol, 1× MEM nonessential amino acids (Mediatech), and 1× sodium pyruvate (Mediatech). To assess mTORC1 activity after stimulation, cells were fixed and permeabilized using BD Cytofix/Cytoperm buffer (BD Biosciences) for 15 min at room temperature. Cells were subsequently washed with 0.5% Tween-20 in PBS and stained with a p-S6 (S240/244) antibody conjugated to Alexa Fluor 647 (Cell Signaling Technologies).

In Vitro B-Cell Inhibitor Treatment. Where the use of pharmacological inhibitors was indicated, a 1× concentration of inhibitor was added to corresponding wells containing purified B cells and allowed to incubate for 15 min at 37 °C in a tissue culture incubator. Following the incubation time, another 1× concentration of inhibitor was added to each corresponding well, followed by a 2× concentration of stimuli. Well contents were mixed by pipetting following both inhibitor additions. Pharmacological inhibitors were used at the following concentrations: PP242 (10 nM, 100 nM, and 400 nM), AZD8055 (1 nM and 10 nM), INK128 (1 nM, 5 nM, 10 nM, and 50 nM), Ku-0063794 (100 nM and 300 nM), rapamycin (0.02 nM, 0.04 nM, 0.08 nM, 0.1 nM, 0.2 nM, 0.4 nM, 0.8 nM, 1 nM, 5 nM, 10 nM, and 20 nM), Akti (500 nM and 1 μM), GDC-0941 (100 nM and 250 nM), and IC87114 (500 nM and 1 μM).

RNA Extraction, RT, and Quantitative RT-PCR. B-cell RNA was extracted using TRIzol reagent (Invitrogen), followed by organic phase purification with Quick-RNA MiniPrep according to the manufacturer's protocol (Zymo Research). For *Aicda*, purified B cells were stimulated with CD40L plus IL-4 or anti-CD40 plus IL-4 for 66 h. For postrecombination Iμ-Cγ1, B cells were stimulated as stated above. cDNA synthesis was carried out on 500 ng to 1 μg of total RNA using iScript Reverse Transcription Supermix (BioRad) for RT-quantitative PCR (qPCR). Gene expression of postrecombination Iμ-Cγ1 and *Aicda* was performed using iTaq Universal SYBR Green Supermix (BioRad), appropriate primers, and Eppendorf Mastercycler ep realplex2 and realplex 2.2 software. Mouse L32 was used as the housekeeping gene. The ratio of gene expression change was determined by the delta-(delta-Ct) method. The following primers were used for qPCR: Iμ-Cμ forward primer 5′-ACCTGGGAATGTATGGTTGTGGCTT-3′ and reverse primer 5′-TCTGAACCTTCAAGGATGCTCTTG-3′, Iμ-Cγ1 forward primer 5′-ACCTGGGAATGTATGGTTGTGGCTT-3′ and reverse primer 5′-ATGGAGTTAGTTTGGGCAGCA-3′, *Aicda* forward primer 5′-TGCTACGTGGTGAAGAGGAG-3′ and reverse primer 5′-TCCCAGTCTGAGATGTAGCG-3′, and mL32 forward primer 5′-AAGCGAAACTGGCGGAAAC-3′ and reverse primer 5′-TAACCGATGTTGGGCATCAG-3′.

FoxO1/2/3 Deletion and FoxO1 Intracellular Staining. For in vivo deletion, *FoxO1/3/4*$^{fl/fl}$; *Mx1-Cre*$^{+}$ and *FoxO1/3/4*$^{fl/fl}$; *Mx1-Cre*$^{-}$ mice were treated i.p. twice, 4 d apart, with 12.5 mg/kg of polyI:C (Amersham), and mice were killed 48 h after the last polyI:C injection. Spleens were harvested, and B cells were purified as described above. FoxO1-deleted B cells were identified by intracellular staining with a rabbit monoclonal antibody against FoxO1 (C29H4; Cell Signaling Technologies). Briefly, B cells were fixed with 2% (vol/vol) paraformaldehyde for 20 min at room temperature, washed, and then permeabilized for 30 min at room temperature with a solution containing 0.2% saponin, 0.05% Nonidet P-40, and 2% (wt/vol) BSA in PBS (permeabilization buffer). Staining for FoxO1 involved a three-layer staining procedure. First, B cells were stained with anti-FoxO1 antibody, followed by a biotinylated donkey anti-rabbit IgG (Southern Biotech), and, lastly, streptavidin-APC (BioLegend). Fc receptors were blocked with TruStain fcX (BioLegend), and all stains and washes were performed with permeabilization buffer.

NP-Ova Immunization and Transient AZD8055 Treatment. Mice were immunized with NP(18)-OVA (Biosearch Technologies) via i.p. injection. NP(18)-OVA was precipitated with Imject alum (Pierce) at a 1:1 ratio to yield a final concentration of 0.05 mg/mL, and mice were each injected with 100 μL (5 μg of antigen). A boost was given at PID 21. For AZD8055 treatment, mice were dosed p.o. once per day with 100 μL of formulated drug at a concentration of 20 mg/kg for a total of 4 d commencing 1 d before NP(18)-OVA immunization and ending on PID 2. Formulation of AZD8055 has been described previously (31). Mice were bled on PID 14 and PID 21 by lancinating the facial vein with a sterile Goldenrod animal lancet (Medipoint). PID 28 blood was collected by cardiac puncture after mice were euthanized with CO_2 gas. Collected blood was allowed to coagulate at room temperature for 10 min and then spun down, and the clear serum fraction was collected and stored for future use at −80 °C.

B-Cell Culture Supernatant and Serum ELISA. For cell culture ELISA to measure total IgM, supernatants from purified B cells stimulated with LPS were collected after 4 d and diluted 1:20 in 2% (wt/vol) BSA in PBS. Nunc Maxisorp plates (Thermo Fisher) were coated with anti-mouse IgM (RMM-1; BioLegend) at 10 μg/mL in 50 μL of total sample in PBS and allowed to incubate overnight at 4 °C. Diluted supernatant samples were incubated on coated plates for 1 h at 37 °C. HRP-conjugated rabbit anti-mouse IgM secondary antibody (Zymed) was used. For NP-specific antibody titers, dilution series were performed using sera from vehicle-treated mice to find the EC_{50} for the different time points and antibody isotypes. The corresponding dilutions that rendered the EC_{50}s were then used for the antibody ELISAs for all samples. Nunc Maxisorp plates were coated at a concentration of 10 μg/mL in a 50-μL total volume with NP(26)-BSA or NP(5)-BSA (Biosearch Technologies) for high-affinity antibody discrimination. HRP-conjugated rabbit anti-mouse IgM secondary antibody and HRP-conjugated goat anti-mouse IgG1 secondary antibody (Southern Biotech) were used for IgM and IgG1 measurements, respectively.

Flow Cytometry, CFSE Labeling, and Antibodies. Before cell surface staining, cells were incubated with TruStain fcX in FACS buffer (0.5% BSA + 0.02% NaN_3 in 1× HBSS) to block Fc receptors for 10 min on ice. Immunophenotyping of mice was performed on splenocytes after RBC lysis. Staining with antibodies was subsequently performed, also with FACS buffer and on ice for 20 min. Flow cytometry antibodies and other reagents used were as follows: CD4 (OKT4), B220 (RA3-6B2), IgG1 (RMG1-1), PD-1 (29F.1A12), IL-21 (FFA21), and IL-17A (TC11-18H10.1) (all from BioLegend); IgD (11-26c), CD38 (90), IgM (eB121-15F9), CD21 (4E3), and CD93 (AA4.1) (all from eBioscience); NP-phycoerythrin (Biosearch Technologies); and Fas (CD95; clone Jo2), CD138 (281-2), and CXCR5 (2G8) (all from BD Biosciences). CFSE labeling of B cells to track proliferation was performed as described elsewhere (32). Flow cytometric data were analyzed using FlowJo software (TreeStar).

Bacterial Strain and Growth Conditions. Attenuated *Salmonella enterica* serovar Typhimurium strain SB824 (*sptP*::Kan Δ*aroA)* is a derivative of strain SL3261, and it was previously described (33–34). Serovar Typhimurium was routinely incubated aerobically at 37 °C in LB broth (10 g of tryptone, 5 g of yeast extract, and 10 g of NaCl per liter).

Immunization of Mice with Recombinant *Salmonella* and AZD8055 Dosing. Specific pathogen-free female C57BL/6 mice, 6–8 wk old, were purchased from Taconic. For the experiments, animals were housed in groups of five mice under barrier conditions. Mice were immunized via i.p. injection with 5 × 10^3 cfu of the indicated *Salmonella* vaccine strain. Where indicated, mice were dosed with AZD8055 at 10 mg/kg p.o. for a total of 4 d beginning on PID 3.

***Salmonella* FACS.** Attenuated *Salmonella enterica* serovar Typhimurium strain SB824 was grown overnight under static conditions. A total of 1 × 10^9 bacteria were aliquoted out into 1.7-mL microcentrifuge tubes and

washed twice with 0.05% BSA in HBSS. After the last wash, samples were blocked on ice with 100 μL of wash buffer for 30 min. Following the blocking step, samples were washed one more time and stained with 100 μL of mouse serum at a concentration of 1:50 in wash buffer for 1 h on ice. Samples were then washed again and stained 1:100 with α-mouse IgM (A85-1; BD Biosciences), α-mouse IgG3 (R40-82; BD Biosciences), or α-mouse IgG2c (Southern Biotech) for 1 h on ice. Flow cytometric data were analyzed with FlowJo software.

In Vitro T Follicular-Cell Differentiation. Mouse-naive $CD4^+$ T cells and follicular B cells were purified by magnetic separation using appropriate kits from Miltenyi Biotec. $CD4^+$ T cells were incubated with indicated inhibitors for 15 min and then stimulated with α-CD3ε (1 μg/mL, 145-2C11; BioLegend) and follicular B cells for costimulation. To make T follicular-cell skewing media, complete RPMI was supplemented with α-mouse IL-2 (JES6-1A12), IL-4 (11B11), IL-12 (C17.8), and IFN-γ (XMG1.2) (all at 10 μg/mL; eBioscience); anti-mouse TGF-β1 (20 μg/mL, TW7-20B9; BioLegend); and IL-6 (30 ng/mL; BioLegend). Cells were cultured for 5 d, and, where indicated, inhibitors were washed off after 24 h. Six hours before harvest, cells were stimulated with phorbol 12-myristate 13-acetate (PMA) (100 ng/mL; Sigma–Aldrich), ionomycin (1 μM; Sigma–Aldrich), and protein transport inhibitor mixture (1×; eBioscience) before intracellular cytokine expression profiling.

ACKNOWLEDGMENTS. We thank Intellikine for providing INK128, Mark Magnuson for providing rictor-flox mice, Paolo Casali for providing CD40L, Egest Pone and Thach Mai for advice on B-cell differentiation assays, and Stephen McSorley for helpful discussions. This work was supported by Public Health Service NIH Grants P30-CA62203, R03-AI085462 and R21-AI099656 (to D.A.F.), T32-AI060573 (to J.J.L. and L.S.), R01-AI083663 (to M.R.), and R00-CA158461 (to S.M.S.); the Pacific Southwest Regional Center of Excellence (M.R.); and the International Society of Experimental Hematology Eugene Goldwasser Fellowship (to S.M.S.). S.M.S. is an American Society of Hematology Junior Scholar.

1. Limon JJ, Fruman DA (2012) Akt and mTOR in B Cell Activation and Differentiation. *Front Immunol* 3:228.
2. Powell JD, Pollizzi KN, Heikamp EB, Horton MR (2012) Regulation of immune responses by mTOR. *Annu Rev Immunol* 30:39–68.
3. Laplante M, Sabatini DM (2012) mTOR signaling in growth control and disease. *Cell* 149(2):274–293.
4. Guertin DA, et al. (2006) Ablation in mice of the mTORC components raptor, rictor, or mLST8 reveals that mTORC2 is required for signaling to Akt-FOXO and PKCalpha, but not S6K1. *Dev Cell* 11(6):859–871.
5. Jacinto E, et al. (2006) SIN1/MIP1 maintains rictor-mTOR complex integrity and regulates Akt phosphorylation and substrate specificity. *Cell* 127(1):125–137.
6. Zhang S, et al. (2013) B cell-specific deficiencies in mTOR limit humoral immune responses. *J Immunol* 191(4):1692–1703.
7. Lee K, et al. (2013) Requirement for Rictor in homeostasis and function of mature B lymphoid cells. *Blood* 122(14):2369–2379.
8. Aagaard-Tillery KM, Jelinek DF (1994) Inhibition of human B lymphocyte cell cycle progression and differentiation by rapamycin. *Cell Immunol* 156(2):493–507.
9. Janes MR, et al. (2010) Effective and selective targeting of leukemia cells using a TORC1/2 kinase inhibitor. *Nat Med* 16(2):205–213.
10. Keating R, et al. (2013) The kinase mTOR modulates the antibody response to provide cross-protective immunity to lethal infection with influenza virus. *Nat Immunol* 14(12):1266–1276.
11. Janes MR, Fruman DA (2010) Targeting TOR dependence in cancer. *Oncotarget* 1(1):69–76.
12. Wander SA, Hennessy BT, Slingerland JM (2011) Next-generation mTOR inhibitors in clinical oncology: How pathway complexity informs therapeutic strategy. *J Clin Invest* 121(4):1231–1241.
13. Xu Z, Zan H, Pone EJ, Mai T, Casali P (2012) Immunoglobulin class-switch DNA recombination: Induction, targeting and beyond. *Nat Rev Immunol* 12(7):517–531.
14. Zhang TT, Makondo KJ, Marshall AJ (2012) p110δ phosphoinositide 3-kinase represses IgE switch by potentiating BCL6 expression. *J Immunol* 188(8):3700–3708.
15. Zhang TT, et al. (2008) Genetic or pharmaceutical blockade of p110delta phosphoinositide 3-kinase enhances IgE production. *J Allergy Clin Immunol* 122:811–819 e812.
16. Chresta CM, et al. (2010) AZD8055 is a potent, selective, and orally bioavailable ATP-competitive mammalian target of rapamycin kinase inhibitor with in vitro and in vivo antitumor activity. *Cancer Res* 70(1):288–298.
17. Willems L, et al. (2012) The dual mTORC1 and mTORC2 inhibitor AZD8055 has anti-tumor activity in acute myeloid leukemia. *Leukemia* 26(6):1195–1202.
18. Rolf J, et al. (2010) Phosphoinositide 3-kinase activity in T cells regulates the magnitude of the germinal center reaction. *J Immunol* 185(7):4042–4052.
19. Cunningham AF, et al. (2007) Salmonella induces a switched antibody response without germinal centers that impedes the extracellular spread of infection. *J Immunol* 178(10):6200–6207.
20. Matsiota-Bernard P, Mahana W, Avrameas S, Nauciel C (1993) Specific and natural antibody production during Salmonella typhimurium infection in genetically susceptible and resistant mice. *Immunology* 79(3):375–380.
21. Haynes L, Eaton SM, Burns EM, Randall TD, Swain SL (2003) CD4 T cell memory derived from young naive cells functions well into old age, but memory generated from aged naive cells functions poorly. *Proc Natl Acad Sci USA* 100(25):15053–15058.
22. Dengler HS, et al. (2008) Distinct functions for the transcription factor Foxo1 at various stages of B cell differentiation. *Nat Immunol* 9(12):1388–1398.
23. Sykes SM, et al. (2011) AKT/FOXO signaling enforces reversible differentiation blockade in myeloid leukemias. *Cell* 146(5):697–708.
24. Tothova Z, et al. (2007) FoxOs are critical mediators of hematopoietic stem cell resistance to physiologic oxidative stress. *Cell* 128(2):325–339.
25. Omori SA, et al. (2006) Regulation of class-switch recombination and plasma cell differentiation by phosphatidylinositol 3-kinase signaling. *Immunity* 25(4):545–557.
26. Jiang Q, et al. (2011) mTOR kinase inhibitor AZD8055 enhances the immunotherapeutic activity of an agonist CD40 antibody in cancer treatment. *Cancer Res* 71(12):4074–4084.
27. Amiel E, et al. (2012) Inhibition of mechanistic target of rapamycin promotes dendritic cell activation and enhances therapeutic autologous vaccination in mice. *J Immunol* 189(5):2151–2158.
28. Janes MR, Fruman DA (2009) Immune regulation by rapamycin: moving beyond T cells. *Sci Signal* 2(67):pe25.
29. Sengupta S, Peterson TR, Laplante M, Oh S, Sabatini DM (2010) mTORC1 controls fasting-induced ketogenesis and its modulation by ageing. *Nature* 468(7327):1100–1104.
30. Shiota C, Woo JT, Lindner J, Shelton KD, Magnuson MA (2006) Multiallelic disruption of the rictor gene in mice reveals that mTOR complex 2 is essential for fetal growth and viability. *Dev Cell* 11(4):583–589.
31. Houghton PJ, et al. (2012) Initial testing (stage 1) of the mTOR kinase inhibitor AZD8055 by the pediatric preclinical testing program. *Pediatr Blood Cancer* 58(2):191–199.
32. Donahue AC, Fruman DA (2003) Proliferation and survival of activated B cells requires sustained antigen receptor engagement and phosphoinositide 3-kinase activation. *J Immunol* 170(12):5851–5860.
33. Rüssmann H, et al. (1998) Delivery of epitopes by the Salmonella type III secretion system for vaccine development. *Science* 281(5376):565–568.
34. Kaniga K, Uralil J, Bliska JB, Galán JE (1996) A secreted protein tyrosine phosphatase with modular effector domains in the bacterial pathogen Salmonella typhimurium. *Mol Microbiol* 21(3):633–641.
35. Hoiseth SK, Stocker BA (1981) Aromatic-dependent Salmonella typhimurium are nonvirulent and effective as live vaccines. *Nature* 291(5812):238–239.
36. Donahue AC, Fruman DA (2007) Distinct signaling mechanisms activate the target of rapamycin in response to different B-cell stimuli. *Eur J Immunol* 37(10):2923–2936.